Chinese Chemical Letters 35 (2024) 109582

Contents lists available at ScienceDirect

Chinese Chemical Letters

journal homepage: www.elsevier.com/locate/cclet

Sn-fused perylene diimides: Synthesis, mechanism, and properties

Wenzhong Zhang, Zirui Yan, Lingcheng Chen*, Yi Xiao*

State Key Laboratory of Fine Chemicals, Dalian University of Technology, Dalian 116024, China

ARTICLE INFO

Article history:
Received 16 August 2023
Revised 17 January 2024
Accepted 28 January 2024
Available online 1 February 2024

Keywords:
Functional dyes
Perylene diimides
Organometallic heterocyclics
Hyperconjugation
Triplet state

ABSTRACT

The first example of metal Sn-fused perylene diimides (**PDI**) derivative (**Sn-PDI**) was designed, synthesized, and investigated. To obtain this type compound, a simple one-pot synthesis, named stannylative cycloaddition reaction, has been successfully developed *via* a palladium-based catalyst system. The novel mechanism exhibits that the reaction experiences oxidative addition, Pd-cyclization, stannylation, Pd-Sn-cyclization, and reductive elimination processes successively. This stannylative cycloaddition does realize unique σ-π hyperconjugation effect and therefore significantly influencing on the photophysical, electrochemical and excited state properties. Compared with those of **PDI**, both of the absorption and fluorescence spectra of **Sn-PDI** display large red-shifts over 20 nm. The electron energy levels of **Sn-PDI** have changed with an uncommon regulation. And **Sn-PDI** gives a considerably raised highest occupied molecular orbital (HOMO) level of -6.00 eV More importantly, the singlet excitons of **Sn-PDI** could efficiently intersystem cross (ISC) into triplet state with a long lifetime of 17.8 μs, which is far longer than that (4.4 ns) of **PDI**.

Due to excellent physical and chemical properties, perylene diimides (**PDI**) have attracted considerable attention not only in traditional dye industries [1,2], but also in modern functional dye fields [3–9]. To obtain the enlarged conjugations of **PDI** derivatives, the two adjacent *bay*-positions of **PDI** could experience (4 + 2) or (4 + 1) cycloaddition reactions to generate the six- or five-membered heterocyclics, respectively [10–15]. Up to now, there are a number of five-membered **PDI** derivatives that are based on heteroatoms of O, S, Se, Te, N, C, or Si, respectively (Fig. 1a). And the different heteroatoms have undoubtedly changed the physical and chemical properties of the parent **PDI** [10–15]. However, all reported five-ring fused **PDI** derivatives are based on the non-metal atoms and there is no example of metal-fused **PDI** derivatives. As we know, the metal atom plays a crucial part in determining the intrinsic properties in the organometallic heterocyclics. Therefore, developing metal-fused **PDI** derivatives and exploring their unusual properties are particularly important.

Stannoles, as a kind of main-group-metal five-membered heterocyclic compounds, have been served as functinonal materials for optoelectronic devices [16,17]. Structurally, stannoles can form the hyperconjugation system between the π-orbitals inside the dienyl ring and the σ-orbitals of the Sn-R bonds and thus giving some unique organometallic properties, such as unusual broad and long-wavelength absorption, changing the electron energy levels greatly, and long lifetime of exciton [18,19]. To realize metal-fused **PDI** derivatives, we consider incorporating a similar structure of stannole into the large conjugated skeleton of perylene unit. And we believe that the introduction of the stannylative cycloaddition would influence the properties of **PDI** dramatically.

With this research interest, in this work, we demonstrated a novel metal Sn-fused **PDI** derivative (**Sn-PDI**), *via* a one-pot synthesis of Pd-catalyzed system from the reactants of monobrominated **PDI** precursor (**Br-PDI**) and hexabutylditin (Fig. 1c). Due to the construction of the hyperconjugation system caused by the fusion of heavy-metal Sn atom, **Sn-PDI** exhibits large red-shifts of absorption and fluorescence spectra. What is more, besides of high fluorescence quantum yield of 0.64, the singlet excitons of **Sn-PDI** could efficiently intersystem cross (ISC) into triplet state with a long lifetime of 17.8 μs.

In the light of electronegativity, size, and polarizability of the heavy-metal Sn, almost all synthesis of stannoles is utilized by the metal-exchange reactions of Li-based reagents (Fig. 1b) [20–24]. And even so, when the aryl halides own large conjugated skeletons, the current strategies are limited to form the stannylative cycloadditions because of smaller electronegativity of Sn and dynamics factors. For instance, using classic synthetic method of Li-based reagent, Kurita *et al.* had synthesized dinaphtho-siloles and -germoles, but failed in dinaphtho-stannole [25]. For the **PDI** structure, due to the intolerance of the imide to Li-based reagents, the previous synthetic techniques cannot be used for synthesizing the stannylative cycloaddition **PDI** derivatives. Therefore, we should

* Corresponding authors.
E-mail addresses: lcchen@dlut.edu.cn (L. Chen), xiaoyi@dlut.edu.cn (Y. Xiao).

https://doi.org/10.1016/j.cclet.2024.109582
1001-8417/

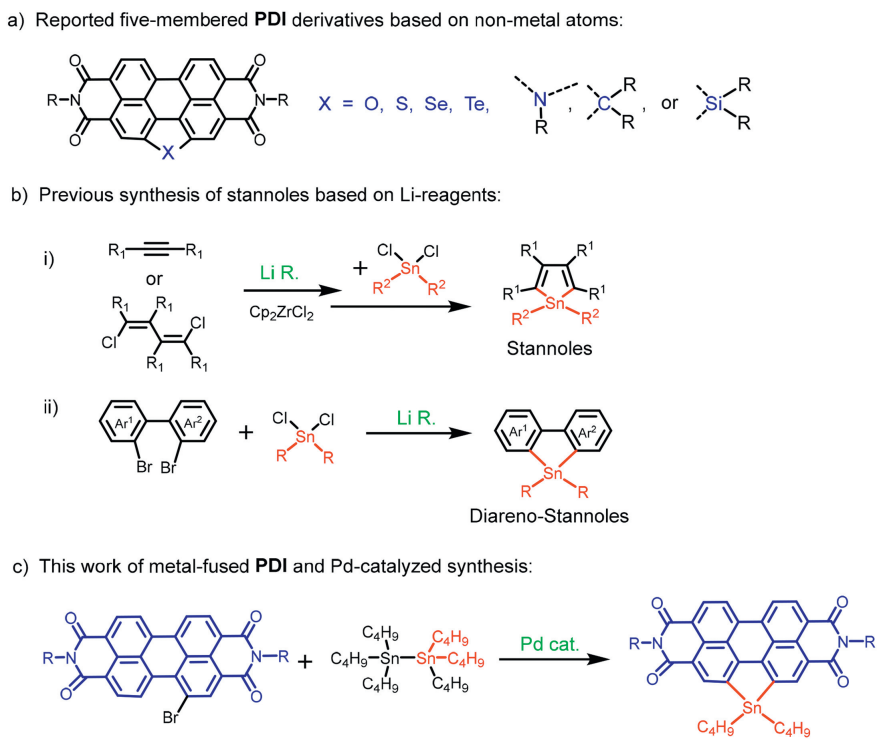

Fig. 1. Background of the five-membered ring fused **PDI** derivatives based on non-metal atoms (a), synthetic approaches of stannoles (b), and our work (metal-fused **PDI** and its Pd-based catalytic reaction) (c).

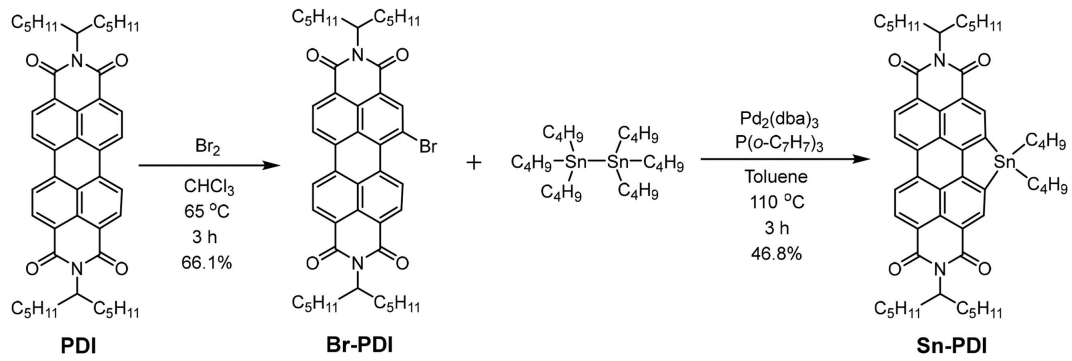

Scheme 1. The synthetic route of **Sn-PDI**.

develop a new method to synthesize it. As shown in Scheme 1, we firstly synthesized the reaction intermediate of **Br-PDI** with a high yield of 66.1%. Then using tris(dibenzylideneacetone)dipalladium ($Pd_2(dba)_3$) and tris(2-methylphenyl)phosphine as the catalytic system in toluene at 110 °C, we have successfully obtained the desired stannylative cycloaddition compound **Sn-PDI** with a yield of 46.8% in a one-pot synthesis. In addition, **Sn-PDI** exhibits high air stability and water insensitivity that could be purified by silica gel column chromatography. As a result, the purified compound was isolated and characterized with ^{1}H NMR spectra. As shown in Fig. 2a and Fig. S6 (Supporting information), **Sn-PDI** gives the poor proton splittings at room temperature, while the splittings of ^{1}H NMR became well-defined when the temperature of the $CDCl_3$ solution rises to 50 °C, which makes the target structure more clear (Fig. 2b and Fig. S7 in Supporting information). The two broad signals of 8.88 and 8.84 ppm for the hydrogens "a" at room temperature (Fig. 2a) coalesce into a sharper singlet at 50 °C (Fig. 2b), which indicates the occurrence of a dynamic conformational process. This dynamic behavior likely involves ring flipping in the stannole system, leading to distinct environments and separate signals for the supposedly equivalent hydrogens "a". To again confirm the molecular structure, besides of the ^{1}H NMR, the characterizations of ^{13}C, ^{119}Sn-NMR and MALDI-TOF/HRMS were also performed and verified the just structure in Supporting information. It should be noted that, the aryl halides, along with hexaalkylditin, could usually convert into the corresponding organotrialkylstannanes through the stannylation [26,27]. However, we did not obtain the organotrialkylstannanes (PDI-$SnBu_3$) in our experiments. The reaction of stannylative cycloaddition is unique and remains an interesting mechanism to study.

To further study this new type reaction, we also synthesized another Sn-fused **PDI** based on different alkane of C5 (Fig. S1 in Supporting information) and then explored the possible mechanism. According to the reported literatures, *via* the palladium-based catalyst, the *o*-halobiaryls can be realized C–H activation and cyclization to generate palladacycles that are usually used as the important intermediates to involve in the following various reactions [28–32]. Especially for **Br-PDI**, the product would be the palladacyclized complex **B** [33], which is the key precatalyst in our mechanism process. Therefore, as shown in Scheme 2, the catalytic cy-

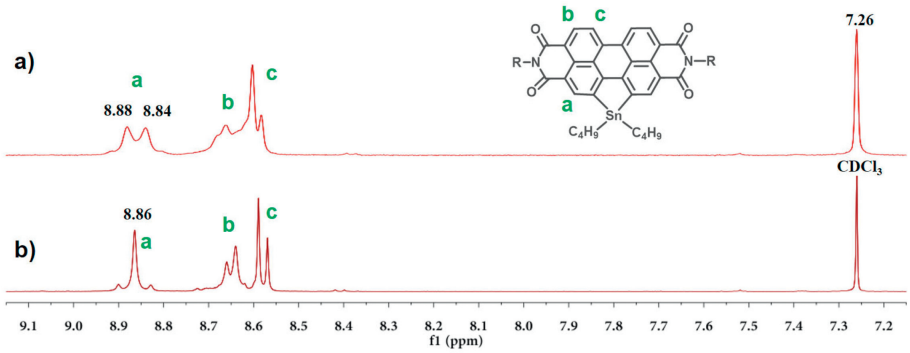

Fig. 2. The ^{1}H NMR spectra at lower fields of **Sn-PDI** at room temperature (a) and 50 °C (b).

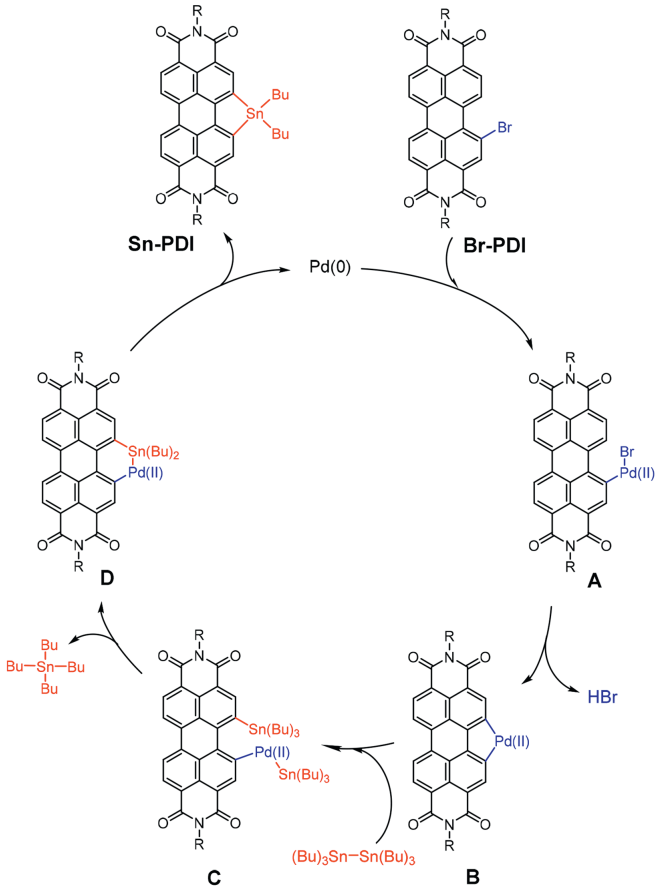

Scheme 2. Proposed mechanism of the Pd-catalyzed stannylative cycloaddition reaction.

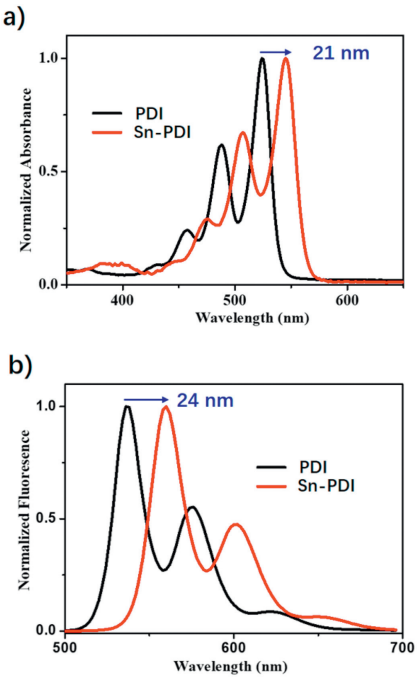

Fig. 3. The absorption (a) and fluorescence (b) spectra of **PDI** and **Sn-PDI**.

cle is as follows: the catalyst Pd(0), with the addition of **Br-PDI**, is oxidized to Pd(II) to form complex **A** firstly. After the intramolecular C–H activation and cyclization at the adjacent *bay*-position of **PDI**, palladacycle **B** is obtained. Next, complex **B** reacts with hexabutylditin to afford dimetallic complex **C**. It should be mentioned that there are two indeterminate reaction pathways to explain the formation of this complex **C** at this stage [31,32]: one is metal-exchange reaction and the other is the oxidation and then reduction process of Pd(II). Afterward, complex **C** is cyclized to produce the Pd-Sn cyclization. At last, product **D** undergoes further reductive elimination to afford the final metal Sn-fused product **Sn-PDI**.

The photophysical properties were investigated in dichloromethane (DCM) solution (10^{-6} mol/L). As shown in Fig. 3a, compared with the ultraviolet visible (UV–vis) absorption spectra of the prototype **PDI**, **Sn-PDI** displays a similar narrow absorption band and an overall red-shifted spectra. And in the spectra, **Sn-PDI** exhibits increased maximum molar extinction coefficient of 7.0×10^4 (6.0×10^4 of **PDI**) and a red-shifted maximum absorption peak of 545 nm (524 nm of **PDI**), which attributes to the introduced σ-π hyperconjugation of the exocyclic C-Sn bonds. Obviously, an analogous trend was found in the fluorescence spectra with the maximum emission of 560 nm for **Sn-PDI**, a red-shift of 24 nm compared with that of **PDI** (Fig. 3b). Meanwhile, **Sn-PDI** emits relatively strong fluorescence in the solution with a fluorescence quantum yield (Φ_F) of 0.64, which is lower than that of **PDI** ($\Phi_F = 0.93$). The reduced Φ_F implies that a portion of singlet excitons may generate the triplet ones *via* the ISC induced by the heavy-metal Sn atom. As shown in Fig. S2 (Supporting information), the average lifetime of the **PDI**'s singlet excitons is 4.4 ns, which is in agreement with the previous report (4.5 ns) [34], while **Sn-PDI** gives a little longer fluorescence lifetime of 5.1 ns. All these results indicate that the cycloaddition of heavy-metal Sn atom has undoubtedly effected the photophysical properties.

The electrochemical properties were performed by the cyclic voltammetry (CV) in DCM with a standard three electrode system. Similar with that of **PDI**, **Sn-PDI** gives two reversible reduc-

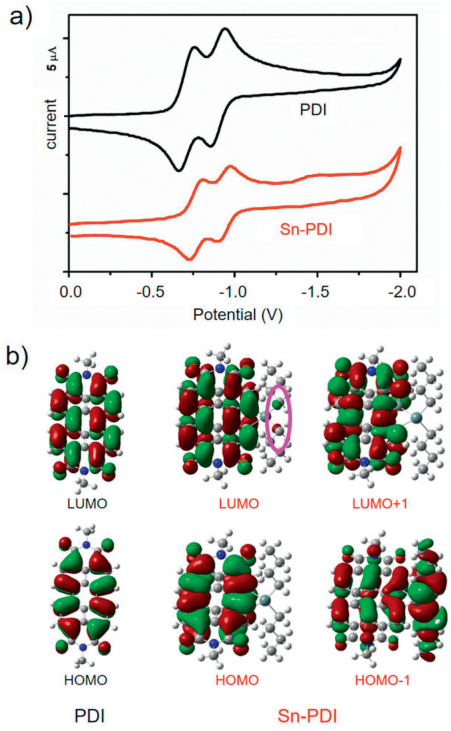

Fig. 4. (a) The cyclic voltammograms in DCM and (b) the theoretical calculations of the electron density distributions of **PDI** and **Sn-PDI**.

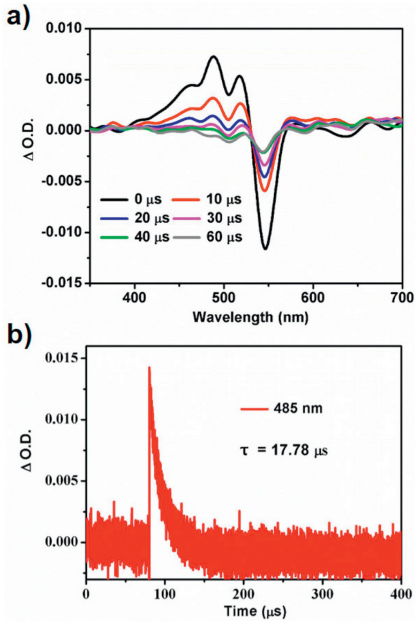

Fig. 5. (a) Nanosecond transient absorption spectra and (b) the decay trace of **Sn-PDI**.

tion waves (Fig. 4a), but the two reduction potentials are more negative. From their first reduction values, the lowest unoccupied molecular orbital (LUMO) energies are estimated to be −3.87 and −3.81 eV for **PDI** and **Sn-PDI**, respectively. Since there is no detectable oxidation wave in the positive potential, the HOMO energies are calculated from the optical energy gaps (E_g) to give the values of −6.14 and −6.00 eV for **PDI** and **Sn-PDI**, respectively. In order to further study how the incorporation of main-group metal Sn influences the electron energy levels, the DFT calculations were performed at the B3LYP/6-31G (d,p) and lanl2dz levels. As shown in Fig. 4b, for **PDI**, the electron density distributions of the HOMO and LUMO are distributed over the conjugated molecule of perylene. For **Sn-PDI**, the electron density of the LUMO is mainly located on the whole conjugation. Besides these, the two σ^*-orbitals connected with Sn are also contributed to the LUMO level with a portion of about 1.04%, which explains the small difference of LUMO levels between the two compounds. Significantly, the electron densities of the HOMO and HOMO-1 are distributed on not only the π-orbitals but also the σ-orbitals with a nonnegligible contribution of about 39.18%, and therefore changing the HOMO level greatly (from −6.14 eV of **PDI** to −6.00 eV of **Sn-PDI** in CV measurement). It is very interesting and important that, our results are absolutely different from the reported stannoles that σ^*-π^* conjugation lowers the LUMO levels due to the enormous effect of the LUMO+1 (which corresponds to the σ^*-orbitals) and has little change on the HOMO levels [17,35-37]. All these phenomena can also be clearly proved by our standard DFT calculation results (Fig. S3 in Supporting information).

To investigate the potential triplet exciton properties, nanosecond transient absorption (nsTA) spectra was measured in DCM solution. As shown in Fig. 5a, the spectra of **Sn-PDI** exhibits narrow ground-state bleaching (GSB) band from 535 nm to 570 nm at $\lambda_{exc} = 532$ nm, and the band-edge (up to 570 nm) is very consistent with that of the absorption spectra (Fig. 3a). Due to the overlap with the excited-state absorption (ESA), GSB in the wavelength range of 450–535 nm is not observed. Clearly, there is a strong ESA from 450 nm to 535 nm, which is assigned to the triplet state absorption [38]. Through the kinetic fitting at 485 nm, triplet state decays with a long lifetime of 17.8 μs (Fig. 5b). For **PDI**, long-lived transient excitons were not traced in nsTA because of the high Φ_F. Then we used **Sn-PDI** as the triplet photosensitizer to oxidize triplet oxygen of singlet oxygen generation to estimate the triplet excition quantum yield (QY) using 1,3-diphenylisobenzofuran (DPBF) as a singlet oxygen scavenger and $Ru(bpy)_3(PF_6)_2$ as the standard (QY: 0.57 in acetonitrile) [39]. As a result, **Sn-PDI** gives a relatively high QY of 0.37 in DCM, which indicates that the singlet excitons could efficiently go into the triplet state from the ISC due to the heavy-atom effect of Sn.

In summary, we have reported the first example of metal tin fused **PDI** derivative **Sn-PDI** in a simple, one-pot synthesis under mild conditions with a high yield of 46.8%. Using $Pd_2(dba)_3$ and tris(2-methylphenyl)phosphine as the catalytic system, the proposed mechanism reveals that **Br-PDI** experiences five successive steps of oxidative addition, Pd-cyclization, stannylation, Pd-Sn-cyclization, and reductive elimination processes to successfully create a new type of stannylative cycloaddition reaction. Due to the construction of the hyperconjugation system, some properties of the new compound have changed greatly. Compared with **PDI**, **Sn-PDI** exhibits large red-shifts of absorption and emission spectra with the maximum peaks of 545 and 560 nm, respectively. And **Sn-PDI** displays different influence trends of raised HOMO and LUMO levlels with −6.00 and −3.81 eV, respectively. More importantly, besides of fluorescence emission with a quantum yield of 0.64, the singlet excitons of **Sn-PDI** could efficiently intersystem cross into the triplet state with a long lifetime of 17.8 μs, which is far longer than that (4.4 ns) of **PDI**. All these unique properties make the new cyclo-Sn fused **PDI** derivatives as the key organic functional dyes for applying in the organic photoelectric devices.

Declaration of competing interest

The authors declare that they have no known competing financial interests or personal relationships that could have appeared to influence the work reported in this paper.

Acknowledgments

This work is supported by the National Natural Science Foundation of China (Nos. 21406027, 21875027, and 22174009), the Medical and Engineering Joint Project of Natural Science Foundation of Liaoning Province (No. 2021-YGJC-17), Supercomputing Center of Dalian University of Technology. And we would like to thank Dr Huihui Wan for assistance with the analysis tests.

Supplementary materials

Supplementary material associated with this article can be found, in the online version, at doi:10.1016/j.cclet.2024.109582.

References

[1] T.C. Patton, Pigment Handbook, Wiley-Interscience, New York, 1973.
[2] E.B. Faulkner, R.J. Schwartz, High Performance Pigments, Wiley-VCH Verlag GmbH & Co. KGaA, Weinheim, 2009.
[3] T. Weil, T. Vosch, J. Hofkens, et al., Angew. Chem. Int. Ed. 49 (2010) 9068–9093.
[4] W. Jiang, Y. Li, Z. Wang, Acc. Chem. Res. 47 (2014) 3135–3147.
[5] D.H. Qu, Q.C. Wang, Q.W. Zhang, et al., Chem. Rev. 115 (2015) 7543–7588.
[6] F. Würthner, C.R. Saha-Möller, B. Fimmel, et al., Chem. Rev. 116 (2016) 962–1052.
[7] Y. Duan, X. Xu, Y. Li, et al., Chin. Chem. Lett. 28 (2017) 2105–2115.
[8] Y. Hou, R. Shi, H. Yuan, et al., Chin. Chem. Lett. 34 (2023) 107688.
[9] S. Zhong, L. Zhu, S. Wu, et al., Chin. Chem. Lett. 34 (2023) 108124.
[10] N. Liang, D. Meng, Z. Wang, Acc. Chem. Res. 54 (2021) 961–975.
[11] V. Sharma, J.D.B. Koenig, G.C. Welch, J. Mater. Chem. A 9 (2021) 6775–6789.
[12] Q. Fan, W. Ni, L. Chen, et al., Chin. Chem. Lett. 31 (2020) 2965–2969.
[13] L. Yang, W. Gu, Y. Chen, et al., Angew. Chem. Int. Ed. 57 (2018) 1096–1102.
[14] Z. Ma, C. Xiao, C. Liu, et al., Org. Lett. 19 (2017) 4331–4334.
[15] K. Chen, N. Xue, G. Liu, et al., Chin. Chem. Lett. 34 (2023) 107884.
[16] J. Linshoeft, E.J. Baum, A. Hussain, et al., Angew. Chem. Int. Ed. 53 (2014) 12916–12920.
[17] S. Urrego-Riveros, I.M. Ramirez y Medina, J. Hoffmann, et al., Chem. Eur. J. 24 (2018) 5680–5696.
[18] R.S. Mulliken, J. Chem. Phys. 7 (1939) 339–352.
[19] I.V. Alabugin, K.M. Gilmore, P.W. Peterson, WIREs Comput. Mol. Sci. 1 (2011) 109–141.
[20] E.H. Braye, W. Hübel, I. Caplier, J. Am. Chem. Soc. 83 (1961) 4406–4413.
[21] P.J. Fagan, W.A. Nugent, J.C. Calabrese, J. Am. Chem. Soc. 116 (1994) 1880–1889.
[22] J. Dubac, A. Laporterie, G. Manuel, Chem. Rev. 90 (1990) 215–263.
[23] X. Yan, C. Xi, Acc. Chem. Res. 48 (2015) 935–946.
[24] J. Krause, K.J. Haack, K.R. Pörschke, et al., J. Am. Chem. Soc. 118 (1996) 804–821.
[25] S. Yasuike, T. Iida, S. Okajima, et al., Tetrahedron 57 (2001) 10047–10053.
[26] D. Azarian, S.S. Dua, C. Eaborn, et al., J. Organometal. Chem. 117 (1976) C55–C57.
[27] H. Azizian, C. Eaborn, A. Pidcock, J. Organometal. Chem. 215 (1981) 49–58.
[28] A. Steffen, R.M. Ward, W.D. Jones, et al., Coord. Chem. Rev. 254 (2010) 1950–1976.
[29] J. Dupont, C.S. Consorti, J. Spencer, Chem. Rev. 105 (2005) 2527–2572.
[30] D. Masselot, J.P.H. Charmant, T. Gallagher, J. Am. Chem. Soc. 128 (2006) 694–695.
[31] G. Shi, D. Chen, H. Jiang, et al., Org. Lett. 18 (2016) 2958–2961.
[32] S. Pan, H. Jiang, Y. Zhang, et al., Org. Lett. 18 (2016) 5192–5195.
[33] G. Gao, N. Liang, H. Geng, et al., J. Am. Chem. Soc. 139 (2017) 15914–15920.
[34] K.M. Felter, R.K. Dubey, F.C. Grozema, J. Chem. Phys. 151 (2019) 094301.
[35] S. Yamaguchi, Y. Itami, K. Tamao, Organometallics 17 (1998) 4910–4916.
[36] M. Hissler, P.W. Dyer, R. Réau, Coord. Chem. Rev. 244 (2003) 1–44.
[37] D. Tanaka, J. Ohshita, Y. Ooyama, et al., Organometallics 32 (2013) 4136–4141.
[38] A.A. Rachford, S. Goeb, F.N. Castellano, J. Am. Chem. Soc. 130 (2008) 2766–2767.
[39] Y. Usui, Chem. Lett. 2 (1973) 743–744.